INTERNAL WWAN/LTE HANDSET ANTENNA INTEGRATED WITH USB CONNECTOR

Kin-Lu Wong and Yu-Wei Chang
Department of Electrical Engineering, National Sun Yat-Sen University, Kaohsiung 804, Taiwan; Corresponding author: wongkl@ema.ee.nsysu.edu.tw

Received 23 July 2011

ABSTRACT: *A new internal eight-band wireless wide area network (WWAN)/long-term evolution (LTE) handset antenna comprising a small antenna ground and two coupled-fed 0.25-wavelength loop antennas disposed on two sides of the antenna ground is presented. In one loop antenna, a chip inductor is embedded to result in dual-resonance excitation of its 0.25-wavelength loop mode and also to adjust the antenna's loading effects on the excited resonant modes at higher frequencies contributed by the other loop antenna. The chip inductor loading greatly helps the proposed antenna in achieving two wide operating bands for the desired WWAN/LTE operation in the 704–960 and 1710–2690 MHz bands. The proposed antenna is especially suitable to be mounted on top of a protruded ground extended from the main ground of the handset to accommodate a universal series bus connector, which serves as a data port of the handset. Details of the proposed antenna are described. Radiation characteristics and specific absorption rate of the antenna are also presented and discussed.* © 2012 Wiley Periodicals, Inc. Microwave Opt Technol Lett 54:1154–1159, 2012; View this article online at wileyonlinelibrary.com. DOI 10.1002/mop.26788

Key words: *handset antennas; multiband antennas; WWAN/LTE antennas; USB connector; coupled-fed loop antennas*

1. INTRODUCTION

With rapid developments in wireless communications, it is becoming a demand that the modern handsets should cover all the operating bands of the wireless wide area network (WWAN) and long-term evolution (LTE) systems. That is, eight-band WWAN/LTE operation in the 704–960 and 1710–2690 MHz should be provided for the embedded internal handset antennas, with the additional requirement that the occupied antenna volume should be as small as possible. For this application, a variety of promising eight-band WWAN/LTE handset antennas have been reported in published papers [1–12]. These WWAN/LTE antennas provide much wider operating bandwidths than the traditional WWAN antennas, which operate in the 824–960 and 1710–2170 MHz bands only [13–23].

Further, close integration of the internal antenna with associated electronic elements in the handset is becoming very attractive to have more flexible disposition of the internal antenna inside the handset. One requirement is for the antenna to integrate with the universal series bus (USB) connector [24], which is usually mounted at the bottom edge of the handset to serve as a data port. When the antenna is also mounted at the bottom edge of the handset, which can lead to decreased specific absorption rate (SAR) values to meet the 1.6 W/kg limit for 1-g head tissue [25–27], the possible coupling between the antenna and the USB connector should be considered such that there is no degradation in the antenna performances. For the reported eight-band WWAN/LTE antennas [1–12], however, there is limited information on this design consideration.

In this article, we present a new internal eight-band WWAN/LTE handset antenna especially suitable to integrate with a USB connector at the bottom edge of the handset. The proposed antenna comprises a small antenna ground and two coupled-fed 0.25-wavelength loop antennas disposed on two sides of the antenna ground. The antenna ground is short circuited to a protruded ground extended from the main ground of the handset to accommodate the USB connector. Because of the short circuiting, the possible capacitive coupling between the proposed antenna and the USB connector can be suppressed, which makes it possible for the antenna to closely integrate with the USB connector without affecting the antenna performances. In one loop antenna, a chip inductor is embedded to result in dual-resonance excitation of its 0.25-wavelength loop mode and also to adjust the antenna's loading effects on the excited resonant modes at higher frequencies contributed by the other loop antenna. With the proposed antenna design, a small antenna volume of $4.8 \times 12 \times 60$ mm^3 (about 3.5 cm^3) for eight-band WWAN/LTE operation in the 704–960 and 1710–2690 MHz bands is achieved. Details of the proposed antenna and its radiation characteristics including the SAR values are presented and discussed.

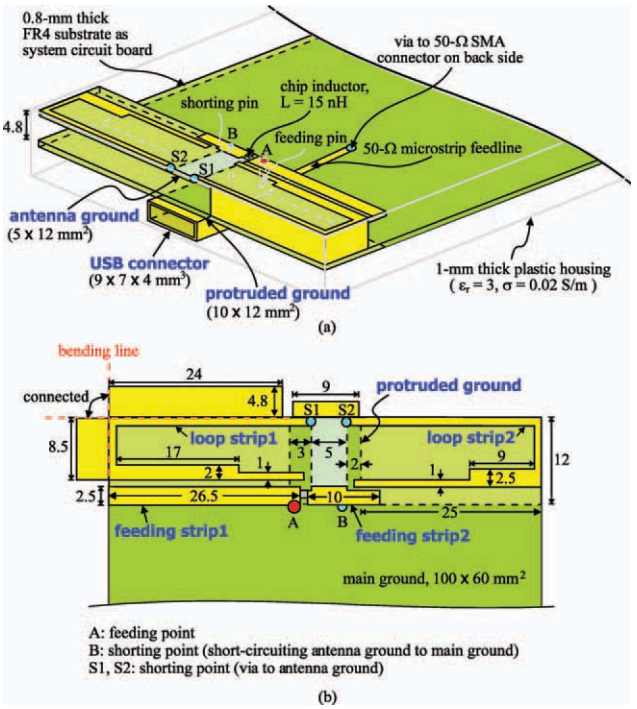

Figure 1 Geometry of the proposed WWAN/LTE handset antenna integrated with a USB connector. [Color figure can be viewed in the online issue, which is available at wileyonlinelibrary.com]

2. PROPOSED ANTENNA

Figure 1 shows the geometry of the proposed WWAN/LTE handset antenna integrated with a USB connector. Photos of the fabricated antenna in the experiment are shown in Figure 2. The antenna is mainly printed on a 0.8-mm thick FR4 substrate (antenna substrate) of relative permittivity 4.4, loss tangent 0.02, and size 12×60 mm^2, which is mounted 4.8 mm above the system circuit board of the handset. That is, the occupied volume is $4.8 \times 12 \times 60$ mm^3 or about 3.5 cm^3 for the proposed antenna. In addition, note that the system circuit board is a 0.8-mm thick FR4 substrate of length 112 mm and width 60 mm in this study. A main ground of size 100×60 mm^2 is printed on the back side of the system circuit board, and there is a protruded ground of size 12×10 mm^2 extended from the main ground. The protruded ground is used to accommodate the USB

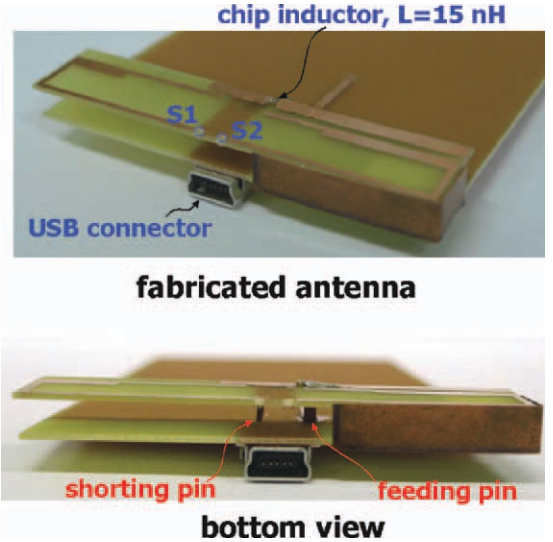

Figure 2 Photos of the fabricated antenna (handset casing not included in the photos). [Color figure can be viewed in the online issue, which is available at wileyonlinelibrary.com]

connector of size 9 × 7 × 4 mm^3 [24]. In the simulation study, the USB connector is modeled as a hollow conducting box of size 9 × 7 × 4 mm^3. In addition, note that the USB connector is 2 mm protruded from the front edge of the protruded ground such that the front end of the USB connector is located at the surface of the handset housing. In the study, a 1-mm thick plastic slab of relative permittivity 3.0 and conductivity 0.02 S/m is used to construct a plastic housing to enclose the antenna and the system circuit board to simulate the handset housing in practical applications.

The proposed antenna comprises an antenna ground and two coupled-fed 0.25-wavelength loop antennas. The antenna ground has a size of 5 × 12 mm^2 and is printed on the back side of the antenna substrate. The antenna ground is short circuited at point B to the protruded ground through a shorting pin and a via-hole in the circuit board. In this case, the antenna ground has about the same electric potential as the protruded ground such that small or negligible capacitive coupling between the antenna and the USB connector disposed on the protruded ground can be obtained [28–30].

The two coupled-fed loop antennas are disposed on the two sides of the antenna ground. The first coupled-fed loop antenna (loop antenna1) consists of a feeding strip1 and a loop strip1, both are printed on the front surface of the antenna substrate, except that the widened metal portion (size 4.8 × 24 mm^2 and 4.8 × 8.5 mm^2) of the loop strip1 is made by a 0.2-mm thick copper plate. The widened metal portion increases the width of the loop strip1 and helps to improve the impedance matching of the excited resonant modes contributed by the loop antenna1. The loop strip1 is short circuited through the via-hole at S1 to the antenna ground and is excited by the feeding strip1 whose front end (point A) is the feeding point of the antenna. In the experiment, a feeding strip of length 4.8 mm connects point A to a 50-Ω microstrip feedline printed on the front surface of the circuit board. The microstrip feedline is further connected to a 50-Ω SMA connector on the back side of the circuit board to test the antenna in the experiment.

A 0.25-wavelength loop resonant mode [27, 31–33] at about 0.75 GHz can be generated by the loop antenna1. In addition, higher order loop resonant modes at about 1.8 and 2.6 GHz are contributed by the loop antenna1. The feeding strip1 is also an efficient radiator [34, 35] and can contribute a 0.25-wavelength monopole resonant mode at about 2.3 GHz. The three resonant modes at about 1.8, 2.3, and 2.6 GHz mainly contributed by the loop antenna1 are formed into a wide upper band for the antenna to cover the desired 1710–2690 MHz band for the GSM1800/1900/UMTS/LTE2300/2500 operation.

The loop antenna2 consists of a feeding strip2, a loop strip2, and an embedded chip inductor of 15 nH. The loop strip2 is short circuited through the via-hole at S2 to the antenna ground and is excited by the feeding strip2. The chip inductor is embedded in the feeding strip2. At higher frequencies, the chip inductor provides a high-inductive reactance, which can be used to adjust the loading effects of the loop antenna2 on the excited resonant modes contributed by the loop antenna1 in the desired upper band. On the other hand, at lower frequencies, this chip inductor leads to a dual-resonance 0.25-wavelength loop resonant mode at about 900 MHz, which combines with the one contributed by the loop antenna1 to form a wide lower band to cover the desired 704–960 MHz band for the LTE700/GSM850/900 operation. The dual-resonance excitation is similar to that obtained using a coupling feed for the shorted monopole antennas [36, 37]. In addition, note that in the proposed antenna, the variations in the widths of the open-end sections of the feeding strip2, the loop strip2, and the loop strip1 are for achieving good capacitive coupling excitation of the two loop antennas.

3. RESULTS AND DISCUSSION

The proposed antenna is fabricated (see Fig. 2) and tested. Results of the measured and simulated return loss are shown in Figure 3. The simulated results are obtained using the commercial available simulation software HFSS version 12 [38]. Agreement between the simulation and measurement is obtained. Two wide operating bands are obtained for the antenna. Over the lower and upper bands, the impedance matching is better than 3:1 VSWR or 6-dB return loss (the widely used design specification for the internal WWAN and LTE handset antennas).

To analyze the operating principle of the proposed antenna, Figure 4 shows a comparison of the simulated return loss for the proposed antenna, the case with the feeding strip only (R1), the case with loop antenna1 only (R2), and the case with loop antenna2 only (R3). For R1, there is a resonant mode excited in the desired upper band, with the impedance matching close to the required 6-dB return loss. When the loop strip1 is added to form R2, a coupled-fed loop antenna is formed and a resonant mode at about 0.75 GHz, which is a 0.25-wavelength loop

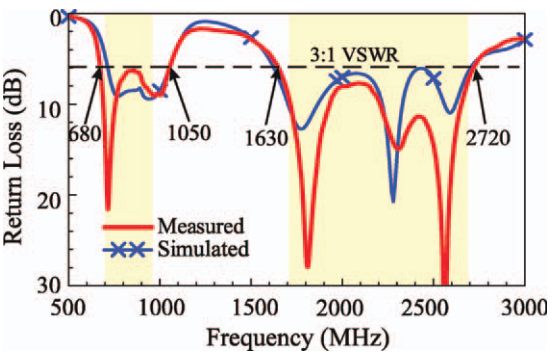

Figure 3 Measured and simulated return loss for the proposed antenna. [Color figure can be viewed in the online issue, which is available at wileyonlinelibrary.com]

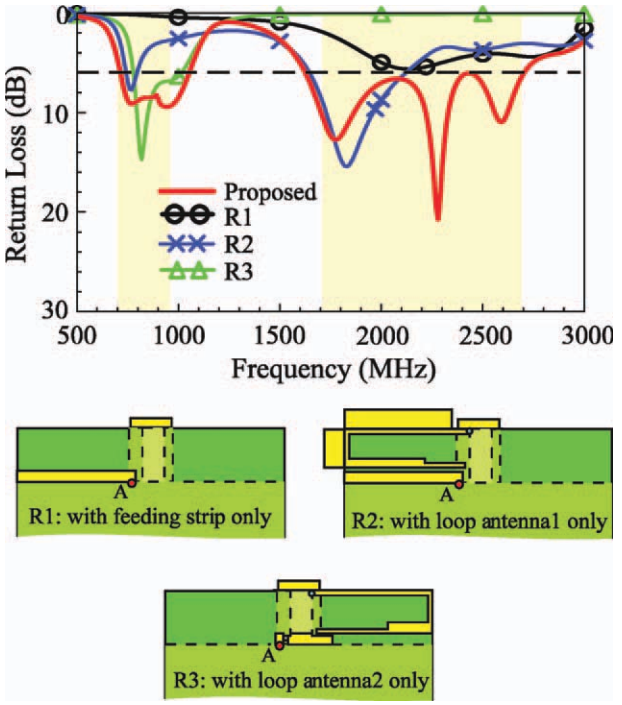

Figure 4 Comparison of the simulated return loss for the proposed antenna, the case with the feeding strip only (R1), the case with loop antenna1 only (R2), and the case with loop antenna2 only (R3). [Color figure can be viewed in the online issue, which is available at wileyonlinelibrary.com]

mode, is excited. In addition, a higher order loop resonant mode at about 1.8 GHz is excited. On the other hand, when there is the loop antenna2 only (R3), a dual-resonance resonant mode at about 900 MHz, which is also a 0.25-wavelength loop mode, is excited. The two 0.25-wavelength loop resonant modes excited by the loop antenna1 and loop antenna2 are combined into a wide lower band to cover the desired 704–960 MHz band. It is also interesting to see that no resonant modes are excited at higher frequencies for R3, which is owing to the chip inductor providing a high-inductive reactance at higher frequencies.

Effects of the chip inductor loaded in the loop antenna2 can be seen more clearly in Figure 5, where the simulated return loss for the proposed antenna and the case using a simple metal

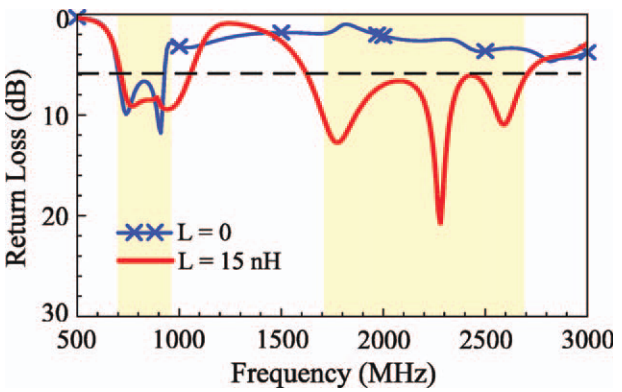

Figure 5 Comparison of the simulated return loss for the proposed antenna and the case using a simple metal strip replacing the chip inductor (i.e., $L = 0$). Other parameters are the same as in Figure 1. [Color figure can be viewed in the online issue, which is available at wileyonlinelibrary.com]

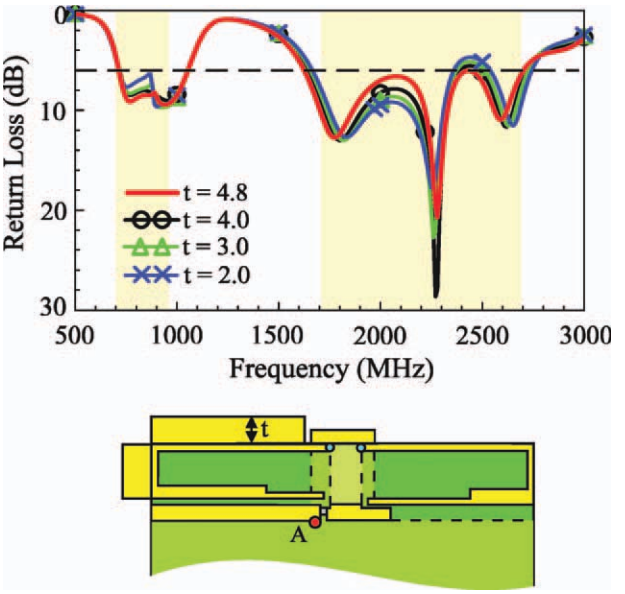

Figure 6 Comparison of the simulated return loss for the proposed antenna as a function of the width t in the loop strip1. Other parameters are the same as in Figure 1. [Color figure can be viewed in the online issue, which is available at wileyonlinelibrary.com]

strip replacing the chip inductor (i.e., $L = 0$) is shown. Without the chip inductor, the impedance matching for frequencies in the desired upper band becomes poor. This indicates the important effects of the chip inductor loaded in the proposed antenna. In addition, the dual-resonance loop mode excited at about 900 MHz contributed by the loop antenna2 becomes a simple single-resonance loop mode, which decreases the bandwidth of the antenna's lower band.

Figure 6 shows the comparison of the simulated return loss for the proposed antenna as a function of the width t in the loop strip1. Results for the width t varied from 2.0 to 4.8 mm are presented. It is seen that the resonant mode contributed by the loop antenna1 at about 0.75 GHz is affected. The two resonant modes at about 1.8 and 2.6 GHz are also shifted to lower frequencies with an increase in the width t, and the impedance

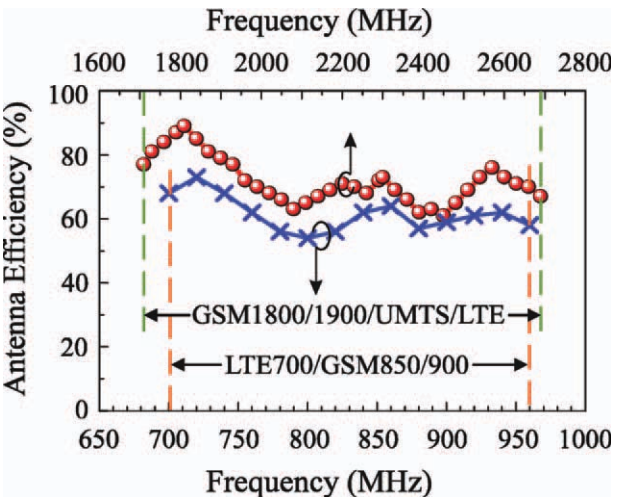

Figure 7 Measured antenna efficiency (mismatching loss included) for the proposed antenna. [Color figure can be viewed in the online issue, which is available at wileyonlinelibrary.com]

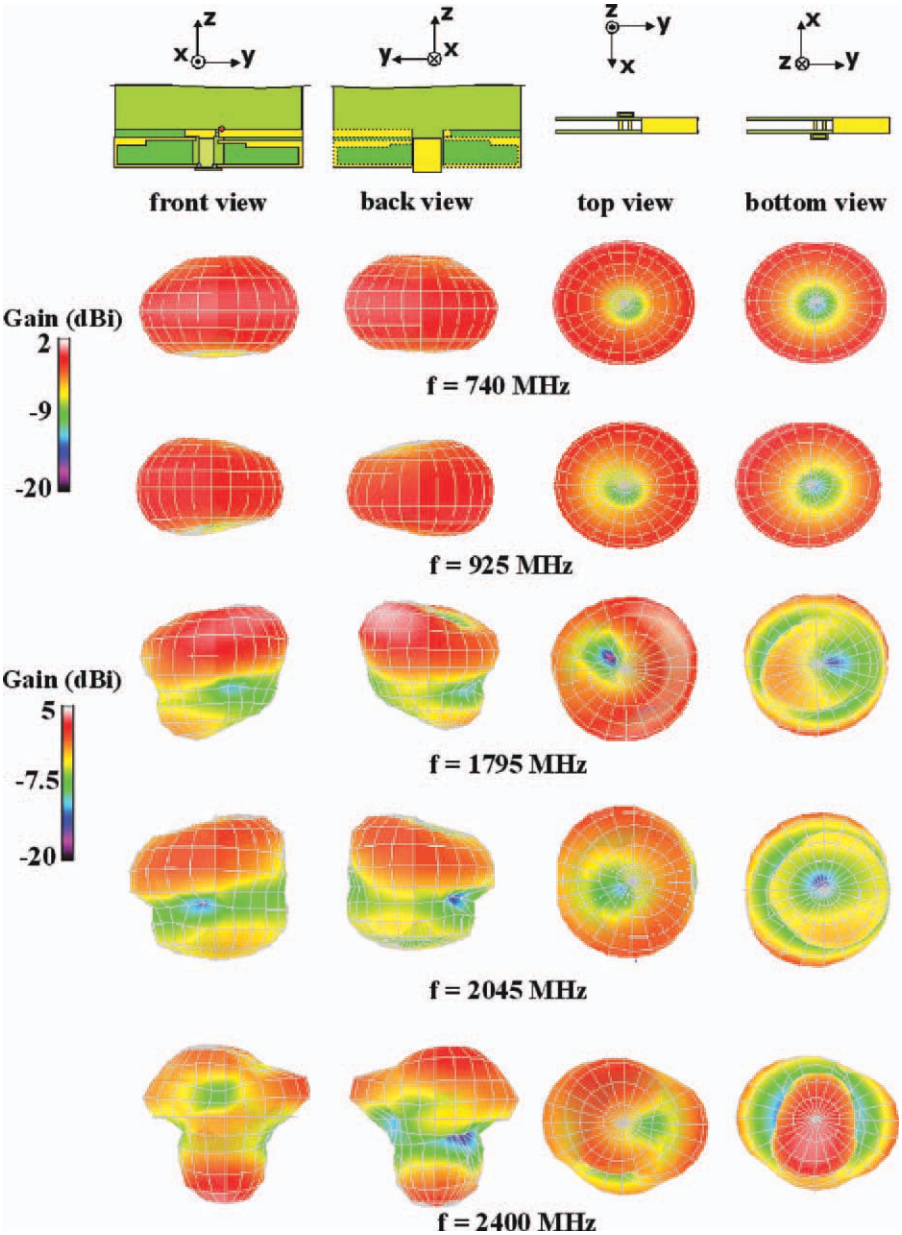

Figure 8 Measured three-dimensional total-power radiation patterns for the proposed antenna. [Color figure can be viewed in the online issue, which is available at wileyonlinelibrary.com]

matching at around 2.5 GHz is also improved. The results also indicate that the three resonant modes at about 0.75, 1.8, and 2.6 GHz are related to the loop antenna1.

Radiation characteristics of the proposed antenna are also studied. Figure 7 shows the measured antenna efficiency of the fabricated antenna. The results are measured in a far-field anechoic chamber, and the measured antenna efficiency includes the mismatching loss. The antenna efficiency varies from about 52 to 72% for frequencies over the lower band, whereas that over the upper band varies from about 60 to 89%. The obtained antenna efficiency is all better than 50%, which is acceptable for practical handset applications. The measured three-dimensional total-power radiation patterns are also presented in Figure 8. Results at five typical frequencies of 740, 925, 1795, 2045, and 2400 MHz are shown. At each frequency, four radiation patterns seen in different directions of the front, back, top, and bottom are shown. At lower frequencies (740 and 925 MHz), dipole-like radiation patterns with omnidirectional radiation in the azimuthal plane (x–y plane) are observed. At higher frequencies (1795, 2045, and 2400 MHz), some dips or nulls in the azimuthal plane of the radiation patterns are seen, which is related to the surface current nulls on the main ground of the handset at higher frequencies. The obtained radiation patterns in general show no special distinctions as compared with those of the reported WWAN/LTE internal handset antennas [1–12].

The SAR results for the proposed antenna are also studied. Figure 9 shows the SAR simulation model and the simulated SAR values for 1-g head tissue. The simulation model is based on the simulation software SEMCAD X version 14 [39]. The simulated SAR values obtained at central frequencies of the eight-operating bands are listed in the table in the figure. The return loss showing the impedance matching level at each testing frequency is also given in the table. The input power for the SAR testing is 21 dBm or 0.125 W for the LTE (740, 2350,

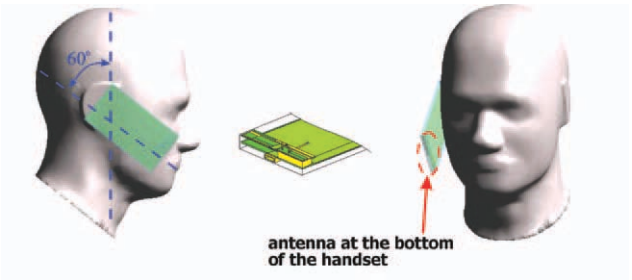

Frequency (MHz)	740	859	925	1795	1920	2045	2350	2595
1-g SAR (W/kg)	0.46	1.05	1.17	0.61	0.57	0.52	0.54	0.52
Input power (Watt in dBm)	21	24	24	21	21	21	21	21
Return loss (dB)	9.1	10.4	10.4	27.0	13.4	10.6	11.0	9.4

Figure 9 SAR simulation model and the simulated SAR values for 1-g head tissue. [Color figure can be viewed in the online issue, which is available at wileyonlinelibrary.com]

2595 MHz), UMTS (2045 MHz), and GSM1800/1900 (1795, 1920 MHz) operations. For the GSM850/900 (859, 925 MHz) operations, the input power is 24 dBm or 0.25 W. The obtained SAR values for 1-g head tissue are all well below the limit of 1.6 W/kg. The results indicate that the proposed antenna is promising for practical handset applications.

4. CONCLUSIONS

A promising internal handset antenna covering the eight-band WWAN/LTE operation and integrated with a USB connector centered below the antenna has been proposed. The antenna has been fabricated and tested. Good radiation characteristics have been obtained for frequencies over the eight-operating bands. Detailed operating principle of the proposed antenna formed by two coupled-fed 0.25-wavelength loop antennas separated by an antenna ground in-between has been studied. Effects of loading a chip inductor in one loop antenna to achieve enhanced bandwidths in both the lower and upper bands of the proposed antenna have been discussed. The antenna occupies a small volume of $4.8 \times 12 \times 60$ mm^3 or about 3.5 cm^3, and the simulated SAR values for 1-g head tissue are well below the limit of 1.6 W/kg. The obtained results indicate that the proposed antenna is promising for practical handset applications.

REFERENCES

1. S.C. Chen and K.L. Wong, Small-size 11-band LTE/WWAN/WLAN internal mobile phone antenna, Microwave Opt Technol Lett 52 (2010), 2603–2608.
2. K.L. Wong and C.T. Lee, Wideband surface-mount chip antenna for eight-band LTE/WWAN slim mobile phone application, Microwave Opt Technol Lett 52 (2010), 2554–2560.
3. K.L. Wong, W.Y. Chen, C.Y. Wu, and W.Y. Li, Small-size internal eight-band LTE/WWAN mobile phone antenna with internal distributed LC matching circuit, Microwave Opt Technol Lett 52 (2010), 2244–2250.
4. K.L. Wong, M.F. Tu, C.Y. Wu, and W.Y. Li, Small-size coupled-fed printed PIFA for internal eight-band LTE/GSM/UMTS mobile phone antenna, Microwave Opt Technol Lett 52 (2010), 2123–2128.
5. S.C. Chen and K.L. Wong, Bandwidth enhancement of coupled-fed on-board printed PIFA using bypass radiating strip for eight-band LTE/GSM/UMTS slim mobile phone, Microwave Opt Technol Lett 52 (2010), 2059–2065.
6. K.L. Wong and W.Y. Chen, Small-size printed loop-type antenna integrated with two stacked coupled-fed shorted strip monopoles for eight-band LTE/GSM/UMTS operation in the mobile phone, Microwave Opt Technol Lett 52 (2010), 1471–1476.
7. F.H. Chu and K.L. Wong, Simple planar printed strip monopole with a closely-coupled parasitic shorted strip for eight-band LTE/GSM/UMTS mobile phone, IEEE Trans Antennas Propag 58 (2010), 3426–3431.
8. C.T. Lee and K.L. Wong, Planar monopole with a coupling feed and an inductive shorting strip for LTE/GSM/UMTS operation in the mobile phone, IEEE Trans Antennas Propag 58 (2010), 2479–2483.
9. S.C. Chen and K.L. Wong, Planar strip monopole with a chip-capacitor-loaded loop radiating feed for LTE/WWAN slim mobile phone, Microwave Opt Technol Lett 53 (2011), 952–958.
10. K.L. Wong and Y.W. Chang, Internal eight-band WWAN/LTE handset antenna using loop shorting strip and chip-capacitor-loaded feeding strip for bandwidth enhancement, Microwave Opt Technol Lett 53 (2011), 1217–1222.
11. F.H. Chu and K.L. Wong, On-board small-size printed LTE/WWAN mobile handset antenna closely integrated with nearby system ground plane, Microwave Opt Technol Lett 53 (2011), 1336–1343.
12. K.L. Wong, T.W. Kang, and M.F. Tu, Antenna array for LTE/WWAN and LTE MIMO operations in the mobile phone, Microwave Opt Technol Lett 53 (2011), 1569–1573.
13. A. Cabedo, J. Anguera, C. Picher, M. Ribo, and C. Puente, Multiband handset antenna combining a PIFA, slots, and ground plane modes, IEEE Trans Antennas Propag 57 (2009), 2526–2533.
14. C.L. Liu, Y.F. Lin, C.M. Liang, S.C. Pan, and H.M. Chen, Miniature internal penta-band monopole antenna for mobile phones, IEEE Trans Antennas Propag 58 (2010), 1008–1011.
15. C.W. Chiu, C.H. Chang, and Y.J. Chi, A compact folded loop antenna for LTE/GSM band mobile phone applications, In: 2010 International Conference on Electromagnetics in Advanced Applications (ICEAA), 2010, pp. 382–385.
16. K.J. Kim, S.H. Lee, B.N. Kim, J.H. Jung, and Y.J. Yoon, Multiband antenna with coupling feed structure for mobile handset applications, In: 2010 IEEE Antennas and Propagation Society International Symposium, Toronto, Canada, 2010, pp. 1–4.
17. R.A. Bhatti and S.O. Park, Hepta-band internal antenna for personal communication handsets, IEEE Trans Antennas Propag 55 (2007), 3398–3403.
18. K.L. Wong and S.C. Chen, Printed single-strip monopole using a chip inductor for penta-band WWAN operation in the mobile phone, IEEE Trans Antennas Propag 58 (2010), 1011–1014.
19. F.H. Chu and K.L. Wong, Simple folded monopole slot antenna for penta-band clamshell mobile phone application, IEEE Trans Antennas Propag 57 (2009), 3680–3684.
20. R.A. Bhatti, Y.T. Im, and S.O. Park, Compact PIFA for mobile terminals supporting multiple cellular and non-cellular standards, IEEE Trans Antennas Propag 57 (2009), 2534–2540.
21. C.H. Chang and K.L. Wong, Printed λ/8-PIFA for penta-band WWAN operation in the mobile phone, IEEE Trans Antennas Propag 57 (2009), 1373–1381.
22. K.L. Wong and L.C. Lee, Multiband printed monopole slot antenna for WWAN operation in the laptop computer, IEEE Trans Antennas Propag 57 (2009), 324–330.
23. K.L. Wong and C.H. Chang, On-board small-size printed monopole antenna integrated with USB connector for penta-band WWAN mobile phone, Microwave Opt Technol Lett 52 (2010), 2523–2527.
24. Universal Serial Bus (USB), Available at: http://www.usb.org/.
25. American National Standards Institute (ANSI), Safety levels with respect to human exposure to radio-frequency electromagnetic field, 3 kHz to 300 GHz, ANSI/IEEE standard C95.1, April 1999.
26. Y.W. Chi and K.L. Wong, Compact multiband folded loop chip antenna for small-size mobile phone, IEEE Trans Antennas Propag 56 (2008), 3797–3803.
27. Y.W. Chi and K.L. Wong, Quarter-wavelength printed loop antenna with an internal printed matching circuit for GSM/DCS/

PCS/UMTS operation in the mobile phone, IEEE Trans Antennas Propag 57 (2009), 2541–2547.
28. C.M. Su, K.L. Wong, C.L. Tang, and S.H. Yeh, EMC internal patch antenna for UMTS operation in a mobile device, IEEE Trans Antennas Propag 53 (2005), 3836–3839.
29. K.L. Wong and C.H. Chang, Surface-mountable EMC monopole chip antenna for WLAN operation, IEEE Trans Antennas Propag 54 (2006), 1100–1104.
30. K.L. Wong, C.H. Chang, and Y.C. Lin, Printed PIFA EM compatible with nearby conducting elements, IEEE Trans Antennas Propag 55 (2007), 2919–2922.
31. Y.W. Chi and K.L. Wong, Very-small-size printed loop antenna for GSM/DCS/PCS/UMTS operation in the mobile phone, Microwave Opt Technol Lett 51 (2009), 184–192.
32. Y.W. Chi and K.L. Wong, Very-small-size folded loop antenna with a band-stop matching circuit for WWAN operation in the mobile phone, Microwave Opt Technol Lett 51 (2009), 808–814.
33. T.W. Kang and K.L. Wong, Internal printed loop/monopole combo antenna for LTE/GSM/UMTS operation in the laptop computer, Microwave Opt Technol Lett 52 (2010), 1673–1678.
34. T.W. Kang, K.L. Wong, L.C. Chou, and M.R. Hsu, Coupled-fed shorted monopole with a radiating feed structure for eight-band LTE/WWAN operation in the laptop computer, IEEE Trans Antennas Propag 59 (2011), 674–679.
35. Y.W. Chi and K.L. Wong, Half-wavelength loop strip fed by a printed monopole for penta-band mobile phone antenna, Microwave Opt Technol Lett 50 (2008), 2549–2554.
36. K.L. Wong and C.H. Huang, Printed PIFA with a coplanar coupling feed for penta-band operation in the mobile phone, Microwave Opt Technol Lett 50 (2008), 3181–3186.
37. K.L. Wong and C.H. Huang, Bandwidth-enhanced internal PIFA with a coupling feed for quad-band operation in the mobile phone, Microwave Opt Technol Lett 50 (2008), 683–687.
38. ANSYS HFSS, Available at: http://www.ansys.com/products/hf/hfss/.
39. SPEAG SEMCAD, Schmid & Partner Engineering AG, Available at: http://www.semcad.com.

NOVEL DESIGN OF COMPACT OPEN-SLOT ANTENNA FOR UWB APPLICATION WITH DUAL BAND-NOTCHED CHARACTERISTICS

A.-F. Sun, Y.-Z. Yin, and Y. Yang
National Laboratory of Antennas and Microwave Technology, Xidian University, Xi'an, Shaanxi 710071, People's Republic of China; Corresponding author: xiansunanfeng@163.com

Received 8 July 2011

ABSTRACT: *In this article, a novel compact UWB antenna with dual band-notched characteristics is proposed. The original UWB antenna is realized by etching an open-slot on the ground plane. The 5.2- and 5.8-GHz WLAN rejected bands are achieved by inserting a slot on the ground plane and a slot-type split ring resonator inside a circular exciting stub on the front side, respectively. The antenna has a compact structure with an area of 16 × 27 mm^2. The small size makes it an excellent candidate for UWB operation. Prototype of the antenna are fabricated and tested. The simulated and measured results show that the proposed antenna achieves a wide impedance bandwidth (VSWR < 2) from 2.92 to over 12 GHz, and the dual rejected bands (VSWR > 2) are 4.85–5.37 GHz and 5.68-5.98 GHz. Radiation patterns and antenna gains are also given in this article. Detailed design steps, parametric studies and experimental results for the antenna are investigated in the following section.* © 2012 Wiley Periodicals, Inc. Microwave Opt Technol Lett 54:1159–1163, 2012; View this article online at wileyonlinelibrary.com. DOI 10.1002/mop.26767

Key words: *open slot antenna; dual band-notched; compact antenna; SRR; UWB*

1. INTRODUCTION

Ultra-wideband communication systems have attracted great attention recently because of their prominent advantages, such as high speed data rate, high precision ranging, and extremely low spectral power density. As one of the main components of UWB systems, UWB antenna has received considerable research. All kinds of configurations have been presented [1–3]. However, to avoid the interferences from the WLAN system operating at 5.15–5.35 GHz and 5.725–5.825 GHz, it's necessary to introduce two notched bands to reject those interferences. The traditional methods include etching slots on the radiating patch [4] or the ground [5, 6], attaching parasitic strips [7, 8]. However, it's difficult to tune the two adjacent notched bands independently because of the space limitation and the strong coupling between the two strips or slots. Recently, some novel resonators have been reported, such as slot-type split ring resonator (SRR) [9] and electromagnetic band gap (EBG) structures [10]. Both structures possess strong resonant characteristics, so they can provide relative narrower notched bandwidths. Because of the sensitivity of the EBG structures to the dimensions, the slot-type SRR is adopted to achieve the desired rejected band.

In this article, a novel compact UWB antenna with dual notched bands is proposed. A slot resonator and a slot-type SRR are adopted to reject the 5.2- and 5.8-GHz WLAN signals, respectively. By varying the dimensions and positions of the two resonators, the center frequencies and the bandwidths of the two adjacent rejected bands can be adjusted easily and independently. Details of antenna design and the results are presented and discussed below.

2. ANTENNA DESIGN

The configuration of the proposed antenna is depicted in Figure 1. The antenna is designed and fabricated on a substrate with relative permittivity of 2.65, thickness of 1 mm, and total area of 16 × 27 mm^2. This antenna is fed by a microstrip-line with width W_f and length L_f, connected to a circular metal patch with of radius R_1 at the microstrip-line end. The ground plane is printed on the opposite side with the dimensions of $W \times L$. To achieve the UWB operating characteristic, an L-shaped open-slot is etched on the ground plane, which occupies an area of $W_{g1} \times L_{g1}$ and $W_{g2} \times L_{g2}$. The distance between the L-shaped slot and the edge of the substrate is L_1. By adjusting the sizes of the structure mentioned above, the UWB operating characteristic can be obtained. The optimized parameters obtained in Ansoft HFSS are as follows: $W = 16$, $L = 27$, $W_f = 2.8$, $L_f = 7.7$, $R_1 = 4.7$, $L_1 = 6.8$, $W_{g1} = 10.8$, $W_{g2} = 4.7$, $L_{g1} = 7.8$, and $L_{g2} = 1.9$ mm.

The desired 5.2- and 5.8-GHz WLAN band-notched characteristics are achieved by placing a slot resonator on the ground plane and a slot-type SRR inside a circular exciting stub on the front side, respectively. The slot-type SRR acts as a resonator, and it can be implemented with a relative small dimension and in a high Q operation. Using the same approach given in Ref. 11, we can obtain the original design dimensions, and then we can adjust the geometry for the final design. The average circumferential length of the SRR plays a dominant role in determining the resonance frequency [12]. The geometry and dimensions of the proposed